Available online at www.sciencedirect.com

ScienceDirect

Procedia CIRP 33 (2015) 527 – 532

www.elsevier.com/locate/procedia

9th CIRP Conference on Intelligent Computation in Manufacturing Engineering - CIRP ICME '14

# Microcutting of multi-layer foils with IR and green ns-pulsed fibre lasers for Li-Ion batteries

Ali Gökhan Demir[a]*, Barbara Previtali[a]

[a]*Department of Mechanical Engineering, Politecnico di Milano, Via La Masa 1, 20156 Milan, Italy*

* Corresponding author. Tel.: +39 02 2399 8538; fax: +39 02 2399 8585. *E-mail address:* aligokhan.demir@polimi.it

**Abstract**

Li-Ion batteries are crucial components in mobile devices that range from cellular phones to electrical vehicles. With the increasing demand in the market for these devices, manufacturers are required to reduce production cycle times. The main components of the Li-Ion batteries are anode and cathode foils, which are cut in required forms by punching. These materials consist of Cu sheets sandwiched between graphite layers for anode, and Al sheets sandwiched between Li metal oxide layers for cathode. In punching, the process quality degrades in time due to tool wear. This eventually causes machine down times for tool repair or change, which can increase the whole process cycle time drastically. Laser remote cutting based on ablation can be adequate solution to substitute the current technology, if the cutting edge quality and productivity can be matched to punching. This paper investigates laser microcutting of Li-Ion battery anode and cathode thin foils with ns-pulsed fibre lasers. These laser sources are cost effective and provide industrially robust operation. Two systems operating with 1 μm and 0.5 μm wavelength and 250 ns and 1 ns pulse durations respectively were compared. The cut kerfs were evaluated in terms of clearance, which is defined as the extent of the exposed middle layer of the sandwich (i.e. Cu or Al) at the laser cut kerf.



Selection and peer-review under responsibility of the International Scientific Committee of "9th CIRP ICME Conference"

*Keywords:* Laser cutting; Laser micro machining; Li-Ion battery

## 1. Introduction

Li-ion batteries are crucial components for improved mobility of electronical devices. Laptop computers, cell phones and hybrid vehicles are only a few examples to products that make use of this technology [1-3]. With increasing demand in energy, their production the production faster and cheaper production becomes evidently important.

Electrodes constitute the key elements of the Li-ion batteries. The electrodes are in the shape of thin sheets and are composed of Cu sheets sandwiched between graphite layers for anode, and Al sheets sandwiched between Li metal oxide layers for cathode. These sheets are conventionally cut by punching on the fly in required shape and size. Due to increasing tool wear, the process quality degrades in time due to tool wear. Eventually, the tool requires change, which causes down time. The repair or replacement of the tool itself is another added cost.

**Nomenclature**

| | |
|---|---|
| $d_0$ | Beam diameter at focal point |
| E | Pulse energy |
| K | Thermal conductivity |
| λ | Laser wavelength |
| τ | Laser pulse duration |
| $T_m$ | Melting point |
| $P_{avg}$ | Average power |
| PRR | Pulse repetition rate |
| v | Scan speed |
| $v_{cut}$ | Maximum cutting speed for a given $P_{avg}$ |
| $v_{max}$ | Maximum cutting speed |
| $w_{kerf}$ | Kerf width |

Laser remote cutting is an emerging process with applications in both macro and micro dimensional ranges [4]. In particular, no process gas is used to expel the material as in the conventional laser cutting. Material removal can be



Selection and peer-review under responsibility of the International Scientific Committee of "9th CIRP ICME Conference"
doi:10.1016/j.procir.2015.06.068

achieved by melting, vaporization or ablation. Pulsed laser sources operating in ns regime are often used for ablation based remote cutting [5-9]. As a matter of fact, ablation based remote microcutting can be an adequate solution to change the current process, since it is a no-contact process without the presence of a physical tool. However productivity and quality of laser cutting should be comparable to punching.

The main defect in laser remote cutting of multi layered li-ion battery electrodes is clearance. As see in Fig. 1, clearance is defined as the extent of the exposed metal plate (i.e. Cu or Al) at the laser cut kerf. Clearance should be minimized, if not totally eliminated for the safe of the Li-ion battery to avoid short circuits. Moreover the exposed metal plate can cut other sheets during stacking and transportation.

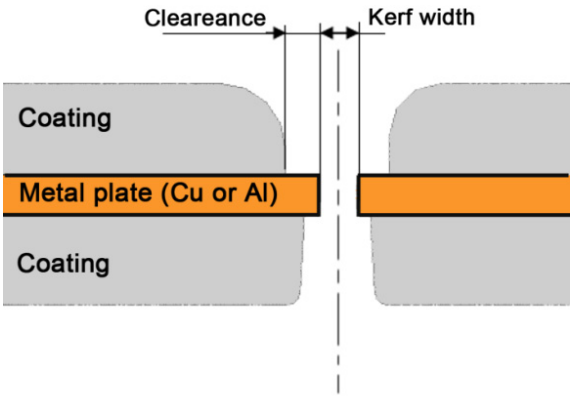


Fig. 1. Schematic representation of a remote laser cut electrode cross section.

In literature only a few number of works explored the possibility of remote laser cutting of Li-ion electrodes [11-14]. Among these, pulsed lasers have been studies sparingly [11], whereas the effect of pulse duration and wavelength appears to be absent. In this work two fibre laser systems operating in IR and green wavelengths are compared. The results are compared to achieve a benchmark in quality and productivity.

## 2. Experimental details

### *2.1. Materials and systems*

Anode and cathode materials were based on thin metallic sheets sandwiched between coating layers. Copper sheets coated with graphite consisted the anode material (140 µm thick). Cathode was formed by Al sheet sandwiched between two layers of Li metal oxide coating (120 µm thick).

Two laser systems operating in ns regime were used to cut both of the electrode materials. A Q-switched fibre laser in fundamental wavelength (λ=1064 nm) with 250 ns pulse duration was used coupled to a scanner head. The scanner head was equipped with an f-theta lens. The calculated beam diameter was 39 µm. The system could reach up to 6000 mm/s scan speed (v). The laser could generate up to 50 W of average power ($P_{avg}$) and operated between 20-80 kHz pulse repetition rate (PRR) range. The second system was a master oscillator power amplifier (MOPA) fibre laser with second harmonic generator (λ=532 nm) and 1 ns pulse duration. The calculated beam diameter of the system was 22 µm. The system was implemented to high precision linear axes, which manipulated the workpiece with a maximum scan speed of 600 mm/s. The laser could generate up to 6 W of average power and

Table 1. General specifications of the used laser systems.

| | IR laser | Green laser |
|---|---|---|
| Brand and model | IPG YLP-1/100/50/50 | IPG YLPG-5 |
| Architecture | Fibre, Q-switched | Fibre, MOPA |
| λ | 1064 nm | 532 nm |
| Max $P_{avg}$ | 50 W | 6 W |
| PRR | 20-80 kHz | 20-300 kHz |
| Max. E | 1020 µJ | 20 µJ |
| τ | 250 ns | 1 ns |
| $d_0$ | 39 µm | 22 µm |

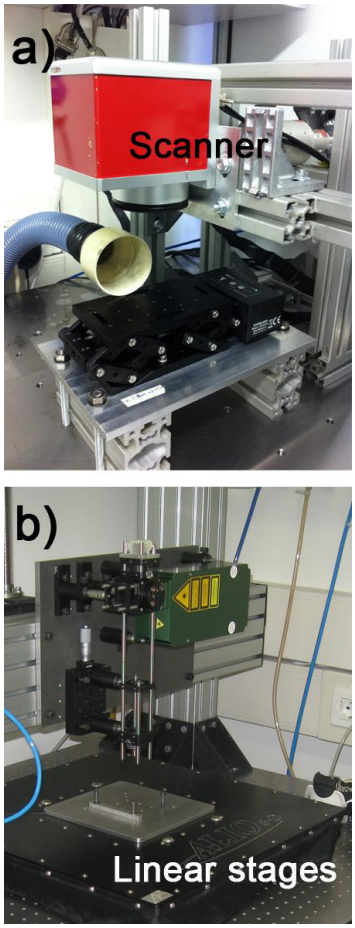


Fig. 2. Laser microcutting systems belonging to a) IR laser, b) green laser.

pulse repetition rate ranged between 20-300 kHz. The general specifications of the two systems are listed in Table 1. Integrated microcutting setups are shown in Fig. 2.

The cutting quality was inspected through optical microscopy and relative measurements were taken on the images obtained via a digital camera. Focus variation microscopy was used for 3D characterization cut kerfs.

*2.2. Experimental plan*

All 4 different laser-material combinations were tested to determine the maximum cutting speed ($v_{cut}$) available for a given $P_{avg}$ level for the highest productivity. Due to the different characteristics of the two laser systems two different processing strategies were adapted.

The IR laser was operated between 20-80 kHz range and different $P_{avg}$ levels. For a fixed $P_{avg}$ cutting speed was varied starting from the maximum achievable value (v=6000 mm/s) and lowered with by steps of 50 mm/s until a complete cut was achieved. On the other hand, for the green laser system was operated with fixed E, and PRR was varied to generate different $P_{avg}$ levels. The relationship between two parameters can be expressed as the following:

$$P_{avg} = E \cdot PRR \quad (1)$$

With the green laser scan speed was varied starting from the maximum achievable value (v=600 mm/s) and lowered with by steps of 5 mm/s until a complete cut was achieved.

## 3. Results and discussion

The results showed that in laser remote cutting with the present pulsed sources until the reach of a limit scan speed the cut evolves from blind grooves to partial cut before reaching a complete cut where the kerf is free of any uncut portions. Fig. 3 compares the blind groove and complete cut conditions on anode. As a matter of fact only complete cuts free of uncut sections are acceptable for the final application. This fact is essentially important to avoid short-circuiting in the manufactured battery.

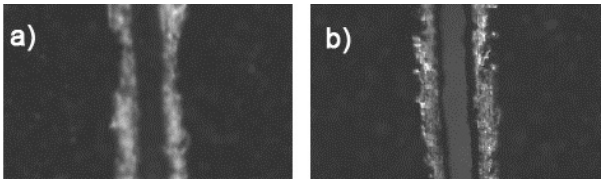


Fig. 3. Evolution of laser remote cutting on anode. a) blind groove, b) complete cut.

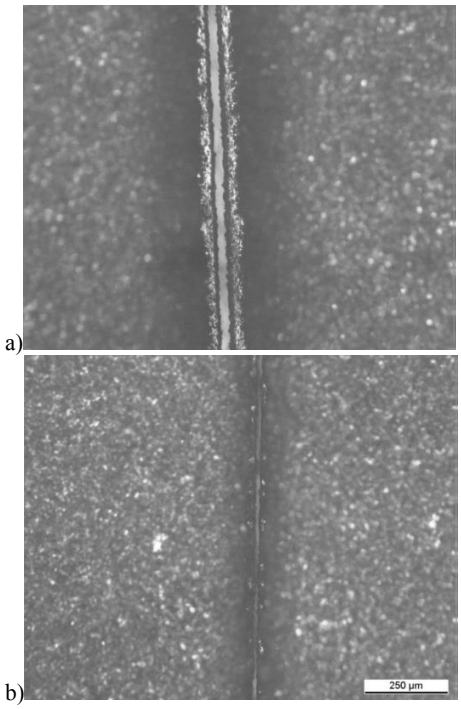


Fig. 4. Comparison of anode kerf quality with the two laser systems: a)IR laser, b) green laser.

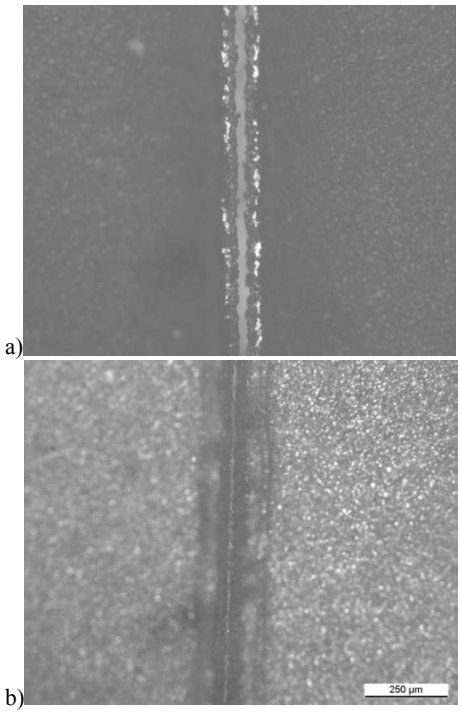


Fig. 5. Comparison of cathode kerf quality with the two laser systems: a)IR laser, b) green laser.

Both productivity and quality in terms of kerf geometry of the two laser sources were considerably different. Figure 4 and 5 report examples of cuts achieved by the systems on anode and cathode with the different laser sources. The clearance is evident on both on anode and cathode with the IR laser sources. This is attributed to the fact that there is a considerable difference in the absorption of the coating and metal layers. As a matter of fact both Cu and Al are highly reflective at the fundamental fibre laser wavelength [15]. On the other hand with the green laser considerable improvement is noticeable. Shorter wavelength improves the absorptivity of the metal layers, whereas the short pulse duration reduces the thermal penetration.

Fig. 6 exhibits the measured kerf width on anode and cathode using the two laser systems. The graph shows the dependence of maximum cutting speed ($v_{cut}$) for the given $P_{avg}$ level as well. Three zones can be identified in the plot: i) zone under the influence of the IR laser, ii) anode cut with green laser and iii) cathode cut with green laser. Over the IR laser zone, the cut kerf has an increasing trend as a function of $P_{avg}$. The measured values are dispersive and similar for both anode and cathode materials. On the other hand, the kerf widths show different behaviour on anode and cathode with the green laser.

In case of the IR laser the dispersed data over the kerf as a function of $P_{avg}$ could be explained by the different clusters of PRR (see Fig. 6). As a matter of fact PRR=20 kHz generated comparable E levels with lower average power ($P_{avg}$). Thus the process can be better described by the pulse energy (E) rather than the average power ($P_{avg}$). Fig. 7 shows the kerf widths generated with the IR laser belonging to anode and cathode as a function of E and PRR. It can be seen that the kerf widths appear to vary between 20-50µm for both materials. Moreover, the kerf width increases faster with the increasing energy level, as expressed by the slope of the regression equation. Such difference can be explained by the lower melting point and higher thermal conductivity of Al ($T_m$=933 K, K=362 W/mK) compared to Cu ($T_m$=1356 K, K=247 W/mK) [16]. Both of the materials are highly reflective to the fundamental fibre laser wavelength. However, at molten stage an increased absorption is expected to occur for both. The lower melting point and higher thermal conductivity facilitates the melt generation, which can absorb more of the laser power. This results in an extended kerf width, especially with larger levels of E.

Fig. 8 shows the kerf width on anode and cathode realized with the green laser as a function of PRR. It can be seen that the kerf width is much smaller for both of the materials. For anode the kerf width results to appear between 10-16 µm without certain dependence over PRR. Small kerf values are the result of small beam diameter and reduced thermal affection provided by the shorter wavelength and pulse duration of the green laser. It should be noted that the machining was carried out with fixed E level. On the other hand, cathode kerf was measured to be lower than 10 µm, hence it is depicted by a limit line on the graph. The absence of a clear trend over the kerf width with fixed E and varying PRR level shows that the kerf width depends on the energy level, which is parallel to the observations made for the IR laser.

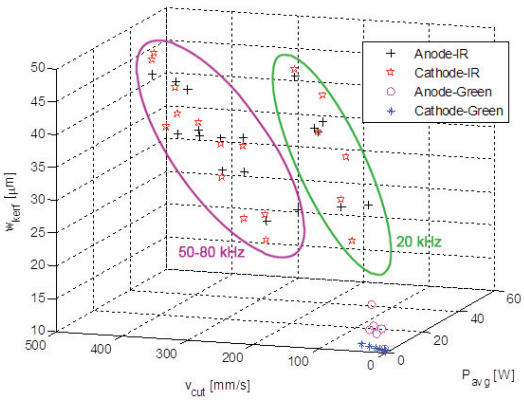


Fig. 6. Kerf width of all material-laser combinations, as a function of $v_{cut}$ and $P_{avg}$.

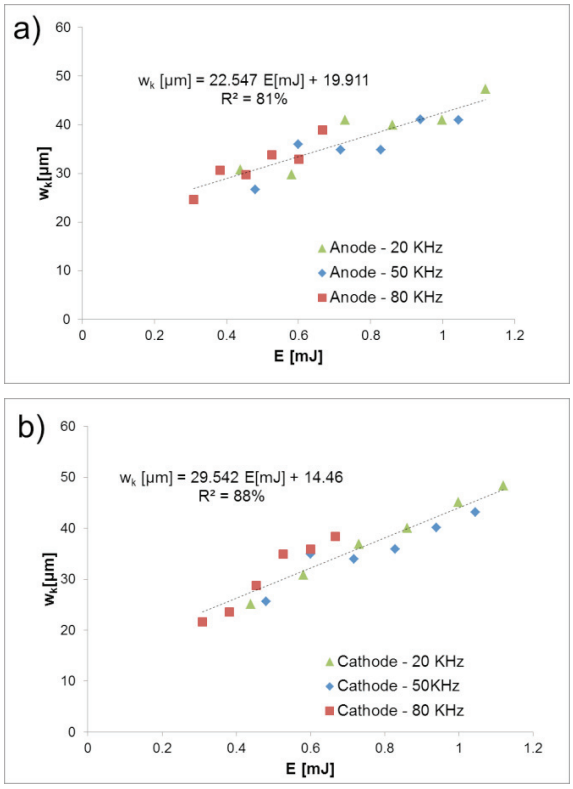


Fig. 7. Kerf width realized with the IR laser as a function of E and PRR on a)anode and b) cathode

Fig. 9 and Fig. 10 on the other hand show the cutting edge morphology for the highest productivity cases of the different laser-material combinations. Highest cutting speed was $v_{max}$=500 mm/s for both electrode materials with the IR laser

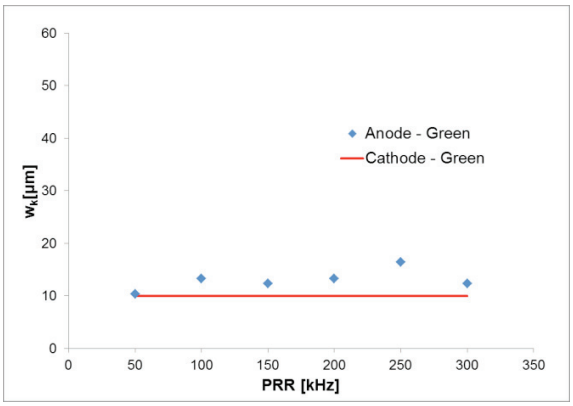


Fig. 8. Kerf width realized with the green laser as a function of PRR on anode and cathode.

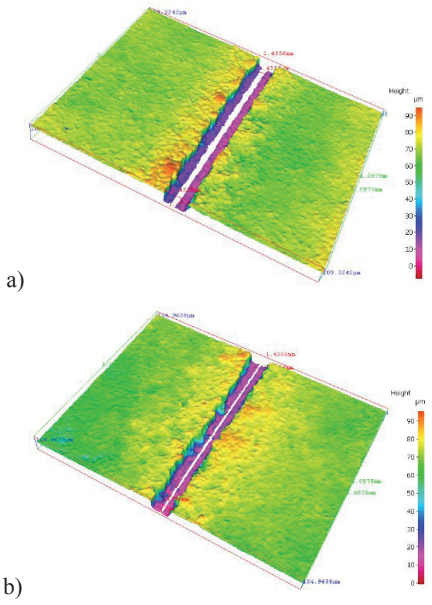


Fig. 9. Comparison of anode kerf geometry of the highest productivity conditions with the two laser systems: a)IR laser, b) green laser.

at highest power level. Kerf width and clearance obtained on anode were 41 µm and 48.8 µm respectively. For cathode they were 43.1 µm and 41 µm. Productivity with the green laser system was relatively low due to the limit in the available power. The maximum cutting speed for anode and cathode was $v_{max}$=40 mm/s and $v_{max}$=75 mm/s respectively, both achieved at the highest average power. With the green laser kerf width and clearance on anode were 12.3 µm and 38 µm respectively. On cathode clearance was not observable at all, while the kerf width was <10 µm. The cut quality morphologies showed a steep fall from the surface to the metal layer for both anode and cathode with the IR laser. A similar morphology with much smaller kerf opening was observable for anode cut with the green laser. In contrast the cut morphology of the cathode with the green laser showed smoothened coating wall without complete detachment.

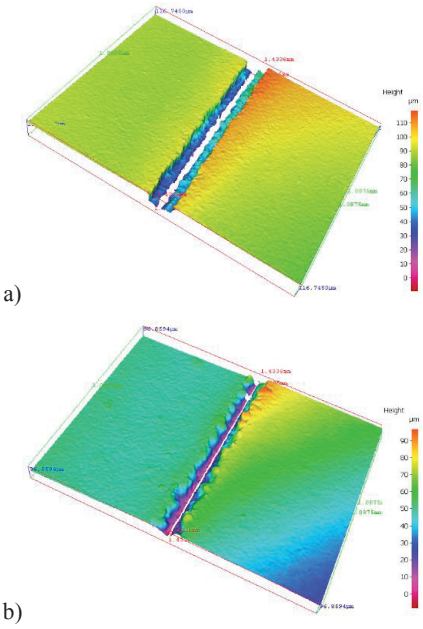


Fig. 10. Comparison of cathode kerf geometry of the highest productivity conditions with the two laser systems: a)IR laser, b) green laser.

## 4. Conclusions

Remote laser microcutting with pulsed fibre laser systems was studied. Two systems differing in wavelength and pulse duration were employed. The initial results show that a great potential is present for manufacturing Li-ion battery electrodes with ablation based cutting. High cutting speed was achieved at 500 mm/s with the high power IR laser system. However, the clearance was found to be around 40 µm. The green laser shows greater promise for improved quality especially on cathode. The clearance was effectively eliminated on cathode with the green laser, whereas the anode clearance remained similar to the one realized with the IR system.

The results confirm that remote laser cutting technology is a viable option for the industrial production of Li-ion battery electrodes. The IR laser already provides high productivity to match the requirements of industrial practice. Ns-pulsed fibre lasers with higher power levels are already available in the market, which can potentially increase the productivity levels to higher than the ones reported here. However, the acceptability of the present clearance extent should be further investigated.

The productivity aspect requires higher average powers for the green laser. With the increasing demand in the market, laser manufacturers are already working on increased power levels

in green laser wavelength, which is a supporting fact for the feasibility of their use in industrial production. Recent developments show increased interest in the development of kW scale power levels for continuous wave green lasers.

Another option for high quality remote cutting of the Li-ion battery electrodes involves the use of industrial scale ultra-short pulsed lasers. The difference in wavelength absorption diminishes, when fs pulses are utilized. Moreover, the cold ablation prevents thermal penetration into the material, which reduces change in machining behavior due to the different thermal properties. However, due to their high capital and operational costs, their applicability in industrial production remains questionable.

## Acknowledgements

The authors gratefully acknowledge the contribution of Mr. Alessandro Colombo, Mr. Nicolò Colombo and Mr. Paolo Colombo in the experimental work.

## References

[1] Peterson S, Whitacre J, Apt J. Net air emissions from electric vehicles: The effect of carbon price and charging strategies. Environmental Science & Technology 2011; 45, 1792–1797

[2] Winter M, Brodd RJ. What Are Batteries, Fuel Cells, and Supercapacitors? Chemical Reviews 2004;104: 4245–4269.

[3] Goodenough JB, Kim Y, Challenges for Rechargeable Li Batteries. Chem. Mater. 2010; 22: 587–603

[4] Lütke M, Mahrle A, Himmer T, Morgenthal L, Beyer E (2008) Remote-cutting – a smart solution using the advantages of high brightness lasers, In Proceedings of 27th International Congress on Applications of Lasers & Electro-Optics ICALEO, 695-702

[5] Zaeh MF, Moesla J, Musiol J, Oefele F. Material Processing with Remote Technology - Revolution or Evolution? Phys Procedia 2010; 5:19–33

[6] Mahrle A, Lütke M, Beyer E. Fibre laser cutting: beam absorption characteristics and gas-free remote cutting. Proc Inst Mech Eng C J Mech Eng Sci 2010; 224(5):1007-1018

[7] Wagner A, Lütke M, Wetzig A, Eng LM. Laser remote-fusion cutting with solid-state lasers. J Laser Appl 2013; 25(5): 052004-1- 052004-8

[8] Fuchs AN, Schoeberl M, Tremmer J, Zaeh MF. Laser Cutting of Carbon Fiber Fabrics. Phys Procedia 2013; 41:372–380

[9] Lütke M, Hauptmann J, Wetzig A, Beyer E. Energetic efficiency of remote cutting in comparison to conventional fusion cutting. J Laser Appl 2012; 24: 022007-1-022007-7

[10] Hock K, Adelmann B, Hellmann R. Comparative study of remote fiber laser and water-jet guided laser cutting of thin metal sheets. Physics Procedia 2012;39:22

[11] Luetke M, Franke V, Techel A, Himmer T, Klotzbach U, Wetzig A, Beyer E. AComparative Study on Cutting Electrodes for Batteries with Lasers. Physics Procedia 2011;12:286-291.

[12] Lee D, Patwa R, Herfurth H, Mazumder J. Computational and experimental studies of laser cutting of the current collectors for lithium-ion batteries J. of Power Sources 2012; 210:327– 338

[13] Lee D, Patwa R, Herfurth H, Mazumder J. High speed remote laser cutting of electrodes for lithium-ion batteries: Anode, Journal of Power Sources 2013; 240: 368-380

[14] Schmieder B, Laser cutting of graphite anodes for automotive lithium-ion secondary batteries: investigations in the edge geometry and heat affected zone. Proc. SPIE 8244, Laser-based Micro- and Nanopackaging and Assembly VI, 2012, 82440R;

[15] Quintino L, Costa A, Miranda R, Yapp D, Kumar V, Kong CJ, Welding with high power fiber lasers – A preliminary study. Materials and Design 2007;28:1231–1237

[16] ASM Handbook, online edition http://products.asminternational.org/hbk/index.jsp (last date of access: 1 April 2014)